King Saud University

Arabian Journal of Chemistry

www.ksu.edu.sa
www.sciencedirect.com

ORIGINAL ARTICLE

Preparation, characterization of some transition metal complexes of hydrazone derivatives and their antibacterial and antioxidant activities

S.A. Aly [a,*], S.K. Fathalla [b]

[a] Department of Environmental Biotechnology, Genetic Engineering and Biotechnology Research Institute, University of Sadat City, Egypt
[b] Chemistry Department, Faculty of Science, Taif University, Saudi Arabia

Abstract   A new series of metal complexes of Pd(II), Cd(II) and Cu(II, I) of polydentate Schiff base ligand (**H₂L**), namely ((Z)-2-(phenylamino)-N'-(thiophen-2-ylmethylene) acetohydrazide) have been prepared. The ligand and its metal complexes have been characterized based on various physico-chemical studies as elemental analyses, molar conductance, spectral (UV–Vis, MS, IR, ^{1}H NMR, ^{13}C NMR and XRD), magnetic moment measurements and thermal studies (TG, DTG). In the view of previous studies, the ligand (**H₂L**) acts as polydentate one and coordinates with metal ions to form all metal complexes. The kinetic and thermodynamic parameters of decomposition process (ΔG, ΔH, ΔS) were calculated. The possible structures of the metal complexes have been computed using the molecular mechanic calculations using the hyper chem. 8.03 molecular modeling program. The calculations are performed to obtain the optimized molecular geometry. The antibacterial study of the selected compounds was assayed against two pathogenic bacteria. Moreover, the complexes (Cu II, I), Cd(II), Pd(II)) and the ligand revealed excellent antioxidant properties and could be useful in fighting the free radicals which occur in close connection with cancerous cells. It was remarkable that the two complexes (Cu II, I) demonstrated stronger antioxidant effects than their parent compounds. It is clear that the new complexes are good active compounds for use in a variety of applications.

© 2019 Published by Elsevier B.V. on behalf of King Saud University. This is an open access article under the CC BY-NC-ND license (http://creativecommons.org/licenses/by-nc-nd/4.0/).

1. Introduction

The development of new derivatives of hydrazone have revealed that they own a wide variety of biological activities such as antimicrobial, anticonvulsant, antidepressant, antiinflammatory, analgesic, antiplatelet, antimalarial, anticancer, antifungal, antitubercular, antiviral and cardio protective

* Corresponding author.
  E-mail address: samar.mostafa@gebri.usc.edu.eg (S.A. Aly).
Peer review under responsibility of King Saud University.

Production and hosting by Elsevier

(kaan et al., 2019). Hydrazones/azomethines imines possess —NHN=CH— and constitute an important class of compounds for novel drug development. A number of researchers have prepared and evaluated the biological activities of hydrazones (Rathinam and Sankaran, 2015; El-Sharief et al., 2013; Loncle et al., 2004; Abdel-Aal et al., 2006; Chavarria et al., 2012; Savini et al., 2004; Bijev, 2006; Imramovsky et al., 2007; Daniela et al., 2019).

Some derivatives of hydrazone such as 2-thaizoylare found to be connected with various biological activities such as anti-inflammatory (Mohamed et al., 2013; Bakr et al., 2012), antiviral (Kesel, 2011), antioxidant (Hasnah et al., 2012; Jaishree et al., 2012), antitumor (Adriana et al., 2015), anticancer (Naidu et al., 2011). Metal complexes of hydrazones are also recognized for their pharmacological activity. Some of them for instance Cu(II) and Ga(III) complexes of hydrazones derivatives are found to be highly cytotoxic to human tumor cell lines (Ferreira et al., 2016; Angel et al., 2014; Recio Despaigne et al., 2012; Dominik et al., 2017; Jiayang et al., 2019).

Diketohydrazides of hydrazine own (C—N) and two (C—O) groups that are considered as electron donors causing the chelating ability of these ligands to different transition metal ions (Shah, 2016; Yousef et al., 2012, 2013, 2014, 2015).

Hydrazones are effective in inhibiting corrosion because their construction contains two nitrogen atoms and an imine bond which act as active adsorption centres (Turuvekere et al., 2016). Previous studies reported the anti-corrosion potential of some new hydrazone derivatives on copper corrosion in NaCl medium and found the maximum percentage inhibition effectiveness (Sherif and Ahmed, 2010). Many combinations of bisisatins were obtained to possess biological activities towards different kinds of targets inside cancer cells (Ibrahim et al., 2016). Addition of certain heterocyclic rings on site 3 of indolin-2- as pyrrole moiety was useful in synthesis of numerous anticancer compounds (Sun and McMahon, 2000; Recio-Despaigne et al., 2012).

We have reported the effect of gamma irradiation on some Ru(II), Pd(II), VO(II) and Hg(II) complexes of (Z)-N-(furan-2-yl)methylene)-2-(phenylamino)acetohydrazide (Samar and Hanaa, 2019). Investigation of synthesized metal complexes was determined by using elemental analyses, magnetic moment, molar conductance, FT-IR, ^{1}H NMR, UV–Vis., spectroscopy and thermal techniques. Spectral, thermal, powder X-ray diffraction patterns (XRD) and surface morphological studies were performed for unirradiated and irradiated metal complexes. Molecular modeling structures, the energies of the highest occupied molecular orbital, energies of the lowest unoccupied molecular orbital, energy gap, the absolute electronegativity, χ, the chemical potential, Pi, the absolute hardness, η and the softness (σ) were calculated for the same compounds. The antibacterial activities of the synthesized compounds were investigated (Samar and Hanaa, 2019).

In the present work, we report the syntheses, spectroscopic characterization and thermal studies of novel Pd(II), Cd(II), Cu(II,I) complexes with 2-phenylamino-N-(thiophene-2-yl) methylene) acetohydrazide ligand. These complexes have been characterized by various physicochemical techniques. The antibacterial and antioxidant activities of the ligand and some selected metal complexes were investigated.

2. Experimental

2.1. Materials and methods

All the chemicals used in preparation of ((Z)-2-phenylamino-N-(thiophene-2-yl) methylene)acetohydrazide ligand (**H₂L**) and Pd(II), Cd(II), Cu(II,I) complexes were of Analar grade and procured from Sigma, Aldrich and Fluka. All reactions were carried out under normal atmospheric conditions.

2.2. Synthesis of Schiff base ligand (H₂L)

((Z)-2-(phenylamino)-N'-(thiophen-2-ylmethylene)acetohydrazide ligand has been prepared as shown in Scheme 1. The anilinohydrazide (1.0 mmol, 1 g) in ethanol (20 mL) was added to an ethanolic solution of 2-thiophene carbaldehyde (1.0 mmol, 0.37 g) (Xavier1 and Srividhya, 2014). The resulting mixture was stirred at room temperature for about 6 h. The buff solid product was collected by filtration and washed several times with ethanol and dried over P_4O_{10}.

2.2.1. [(H₂L)], (M.F.: C₁₃H₁₃N₃OS and M.W.: 259)

Elemental analysis of (**H₂L**) gave, C = 60.0% (60.2), H = 4.70% (5.0) and N = 16.0% (16.2), (where the numbers in parenthesis represent the calculated value from the chemical formula). Electronic absorption spectra of (**H₂L**) in DMF solution, λ_{max}/nm: 250, 325. Selected IR frequencies (KBr disk, cm^{-1}): 3381, 3244, 1628 and 690.

2.3. Synthesis of the metal complexes

Metal complexes were prepared by adding stoichiometric amount of the appropriate metal salt, Na_2PdCl_4, $CdCl_2$, $Cu(ClO_4)_2$, CuCl and CuI in EtOH to (Z)-2-(phenylamino)-N'-(thiophen-2-ylmethylene) acetohydrazide (20 mL) in the same solvent. The reaction mixture was heated with stirring at ca. 60 °C for 6 h. The resulting solids were filtered off, washed several times with EtOH, and dried under vacuum over P_4O_{10}.
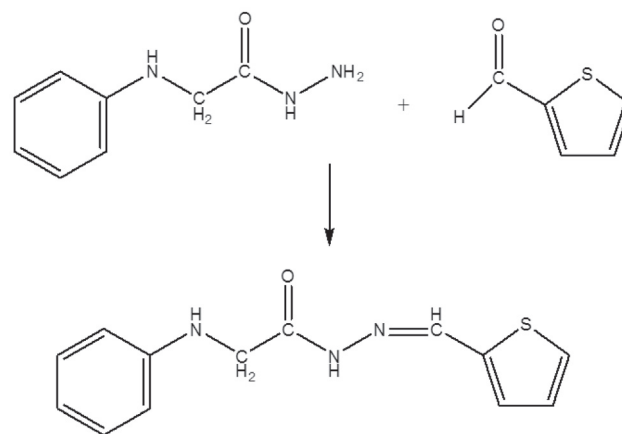
(Z)-2-(phenylamino)-N'-(thiophen-2-ylmethylene)acetohydrazide

Scheme 1   Synthesis of ligand (H₂L).

2.3.1. [Pd(H₂L)(OH)Cl]·1/2H₂O] C₁, (M.F.: C₁₃H₁₅N₃O₁øS Pd and M.W.: 426.5)

Elemental analysis of **C₁** gave; C = 36.5% (36.57), H = 3.20% (3.50), N = 9.80% (9.85), Cl = 8.30% (8.30) and Pd = 24.58% (24.85) (where the numbers in parenthesis represent the calculated value from the chemical formula). Electronic absorption spectra of **C₁** in DMF solution, λ_{max}/nm: 323, 399, 520. Selected IR frequencies (KBr disk, cm^{-1}): 3431, 3194, 3135, 1602, 438 and 512.

2.3.2. [Cd(H₂L)Cl₂], C₂(M.F.: C₁₃H₁₃N₃OSCl₂Cd and M.W.: 442.5)

Elemental analysis of **C₂** gave; C = 35.37% (35.25), H = 3.08% (2.94), N = 9.6% (9.5), Cl = 16.20% (16.00) and Cd = 25.4% (24.5) (where the numbers in parenthesis represent the calculated value from the chemical formula). Electronic absorption spectra of **C₂** in DMF solution, λ_{max}/nm: 316. Selected IR frequencies (KBr disk, cm^{-1}):3413, 3171, 3069, 1707, 427 and 503.

2.3.3. [Cu(H₂L)(HL)·OH] C₃ (M.F.: C₂₆H₂₆N₆O₃S₂Cu and M.W.: 597.5]

Elemental analysis of **C₃** gave; C = 52.60% (52.21), H = 4.50% (4.35), N = 14.30% (14.06) and Cu = 10.56% (10.63) (where the numbers in parenthesis represent the calculated value from the chemical formula). Electronic absorption spectra of **C₃** in DMF solution, λmax/nm: 325, 379, 420 and 615. Selected IR frequencies (KBr disk, cm^{-1}): 3336, 3042, 3019, 1608, 1534, 452, and 575.

2.3.4. [Cu(H₂L)₂Cl]·1/2H₂O] C₄ (M.F.: C₂₆H₂₇N₆ O₂ø S₂ ClCu and M.W.: 626.0]

Elemental analysis of **C₄** gave; C = 49.7% (49.84), H = 4.20% (4.31), N = 13.40% (13.42), Cl = 5.46% (5.67) and Cu = 10.05% (10.14) (where the numbers in parenthesis represent the calculated value from the chemical formula). Electronic absorption spectra of **C₄** in DMF solution, λmax/nm: 338, 389, 440 and 607. Selected IR frequencies (KBr disk, cm^{-1}): 3432, 2923, 1674, 1604, 455, and 511.

2.3.5. [Cu₂(H₂L)₂(HL)(OH)] C₅ (M.F.: [C₃₉H₄₁N₉O₄S₃Cu₂] and M.W.: 938.1]

Elemental analysis of **C₅** gave; C = 50.1% (49.9), H = 4.50% (4.3), N = 13.5% (13.4) and Cu = 14.32% (13.5) (where the numbers in parenthesis represent the calculated value from the chemical formula). Electronic absorption spectra of **C₅** in DMF solution, λmax/nm: 340, 379 and 600. Selected IR frequencies (KBr disk, cm^{-1}): 3444, 3336, 3091, 1606, 1534, 485, and 571.

2.4. Physical measurements

The elemental analyses (C, H, N) were performed at Cairo University, Giza, Egypt using CHNS-932 (LECO) Vario Elemental Analyzer. Metal and halide content were estimated by complexometry using EDTA following standard literature methods (Bassett et al., 1978). The metal content was also confirmed from the thermal results. The Fourier Transform Infrared (FTIR) measurements were performed (4000– 400 cm^{-1}) in KBr discs using Nenexeus-Nicolidite-640-MSA FT-IR, Thermo-Electronics Co. The UV–visible absorption spectra were measured in DMF solution using 4802 UV/vis double beam spectrophotometer. The ^{1}H NMR and ^{13}C NMR spectra have been recorded in DMSO-d_6 as a solvent using Varian Gemini 200 NMR spectrophotometer and Varian-Oxford Mercury at 300 MHz, respectively.

Molar conductivities of complexes were measured at 30 °C in DMF solution (10^{-3}M) using a CON 6000 conductivity meter. Magnetic susceptibilities of the complexes were measured at room temperature by the modified Gouy method using magnetic susceptibility Johnson Matthey Balance. The effective magnetic moments were calculated using the relation $\mu eff = 2.828 (X_mT)^{1/2}$B.M., where X_m is the molar susceptibility corrected for diamagnetism of all atoms in the compounds. Thermal analysis (TG/DTG) was obtained out by using a Shimadzu DTA/TG-50 Thermal Analyzer with heating rate of 10 °C/min in nitrogen atmosphere with a following rate 20 mL/min in the range of ambient temperature up to 800 °C using platinum crucibles. Electro spray mass spectra (ESI–MS) for the complexes were performed at the National Research Center, Egypt by the Thermo Electron Corporation. The electron impact (EI) mass spectrum for the ligand was run on Shimadzu-QP 2010 plus Mass Spectrometer, Micro analytical Laboratory, Faculty of Science, Cairo University, Egypt. X-ray powder diffraction analyses of solid samples were measured using APD 2000 PROModel GNR-X-ray Diffractometerat (NRC, Tanta University, Egypt). X-ray diffractograms gives computer control formally finished by PHILIPS®MPDXPERT X-ray diffratometer ready with Cu radiation CuKα (λ = 1.540 56 Å). The xpertdiffractometer has the Bragg- Brentano geometry. The x-ray tube used was a copper tube operating at 40 KV and 30 mA. The scanning range (2θ) was 5–90° with step size of 0.050° and counting time of 2 s/step. Quartz was used as the standard material to accurate for the instrumental expansion. This identification of the complexes was done by a known method (Harikumaran and Appukuttan, 2012). From the fitidentified Scherrer formula, the average crystallite size (D) is

$$D = (K\lambda/\beta\cos\theta)$$

where λ is the X- ray wavelength in the nanometer, K is factor related to crystallite shape, with a value about 0.9 and ß is the peak width at half maximum height. The value of ß in the 2θ axis of diffraction shape must be in radians. The θ is the Bragg angle and be able to in radians since the Cos θ compatible with the same number.

2.5. Theoretical calculation (molecular modeling)

Molecular modeling was applied to investigate the three dimensional arrangements of atoms in the complexes by employing semi-emperical molecular orbital calculations at the PM3 level provided by the HyperChem program (HyperChem, 2007).

2.6. Biological applications

2.6.1. Antibacterial activity

The *in vitro* antibacterial activity studies were carried out in the department of Microbial Biotechnology, Genetic Engineering and Biotechnology Research Institute, Sadat City University,

Egypt, by using Broth Dilution Method with some alterations (Wikler et al., 2009) to investigate the inhibitory effect of ligand and synthesized complexes (**C₁-C₅**) on the sensitive organisms *Streptococcus pyogenes* as Gram- positive bacterium and *Escherichia coli* as Gram–negative bacterium. Nutrient broth medium was prepared by using Brain Heart Infusion (BHI) broth and distilled water. The test compounds in measured quantities were dissolved in DMSO which has no inhibition activity to get two different concentrations (1 mg/mL, 5 mg/mL) of compounds. The strains selected for the study were prepared in (BHI) broth medium with shaking and autoclaved for 20 min 15 lb of pressure and at 121 °C before inoculation. The bacteria were then cultured for 24 h at 37 °C in an incubator. One ml of the standard bacterial culture was used as inoculation in a nutrient broth. For growth studies, culture of microbial cells were inoculated and grown aerobically in BHI broth for control and along with various concentrations of the test compounds in individual flasks. Growth was calculated turbidometrically at 650 nm using conventional Spectrophotometer, in which turbidity produced is measured by taking absorbance and compared with turbidity produced by control. The growth rate of different bacteria in absence as well as in presence of test compounds was performed for each concentration. Absorption measurements were accomplished by spectrophotometer after 24 and 48 h of incubation to determine the number of viable organisms per milliliter of sample and were used to the calculated the % inhibition (Umit et al., 2018; Abdülmelik et al., 2019; Nuraniye et al., 2019).

2.6.2. Assay for DPPH free-radical scavenging potential

The nitrogen centered stable free radical 2,2′-diphenyl-1-picryl hydrazyl (DPPH) has often been used to characterize antioxidants (Gülçin et al., 2010; Ercan and Ilhami, 2011; Leyla et al., 2015). It is reversibly reduced and the odd electron in the DPPH free radical gives a strong absorption maximum at λ 517 nm, which is purple in colour (Blois, 1958). Each sample at different concentrations (100, 200 and 300 µg) in HPLC methanol was added to the solution [3.9 mL, 0.004% (w/v)] of DPPH⁰ in methanol. The tubes were kept at an ambient temperature for 30 min and the absorbance was measured at λ 517 nm. All tests were performed in triplicate and mean were

calculated. The scavenging activity (SCA) was expressed as a percentage of scavenging activity on DPPH:

$$SCA\% = [(A_{control} - A_{test})/A_{control}] \times 100$$

where $A_{control}$ is the absorbance of the control (DPPH solution without test sample) and A_{test} is the absorbance of the test sample (DPPH solution plus scavenger).

Butylated hydroxyl anisole (BHA) and *tert*-Butylated hydroxyl qunione (TBHQ) were used as positive controls. All tests were run in triplicate and an average was used (Gülçin, 2006a,b; Ak and Gülçin, 2008).

3. Results and discussion

3.1. Physical properties

The purity of the ligand and Pd(II), Cd(II), Cu(II, I) complexes have been checked by TLC. All of the metal complexes are coloured solids except complex C₂, stable towards air, slightly soluble in alcohols, insoluble in most common organic solvents, but soluble in DMF and/or DMSO. The elemental analyses display that, complexes (C₁, C₂) are 1L:1M, while (C₃,C₄) and (C₅) are 2L:1M and 3L:2M stoichiometry, respectively (Table 1). The measured values of the molar conductance of complexes in 10^{-3} M DMF solution at room temperature were in the range of 12–20 (ohm^{-1} cm^2 mol^{-1}). These values reveal that all complexes are non-electrolyte (Bayoumi et al., 2013). The analytical and physical data are compatible with the suggested structures.

3.1.1. ¹H NMR spectrum of the ligand

The ¹H NMR spectrum of the ligand was verified in DMSO-d_6 solution (Fig. 1). The spectrum shows that the different non-equivalent protons resonate at different values of applied field. The ¹H NMR spectrum exhibits one signal at δ 4.14 ppm assigned to —NH of amine protons and the multiple peaks observed in the region of (NH—CH₂) and (OC—NH—CH₂) signals indicate chemically non-equivalent methylene protons. Furthermore, the spectrum displays a multiple signal at δ (6.58–7.63 ppm) assigned to aromatic ring protons. Also, the spectrum depicts signals at δ (8.48, 11.46 and 7.63 ppm) to

Table 1 Analytical and physical data of ligand and its metal complexes.

No.	Compounds	Emperical formula	Color	Mol. wt.	Found (Calc.)% C	H	N	M	Cl	Λ_m
	H₂L	C₁₃H₁₃N₃OS	Buff	259	60.0 (60.23)	4.7 (5.0)	16.00 (16.20)	–	–	–
C₁	[Pd(H₂L)(OH)Cl]·1/2H₂O	C₁₃H₁₅N₃O₁.₉SPd	Yellow	426.5	36.50 (36.57)	3.20 (3.5)	9.80 (9.85)	24.58 (24.85)	8.30 (8.30)	12
C₂	[Cd(H₂L)Cl₂]	C₁₃H₁₃N₃OSCl₂Cd	white	442.5	35.37 (35.26)	3.08 (2.94)	9.60 (9.50)	24.50 (25.40)	16.20 (16.00)	20
C₃	[Cu(H₂L)(HL).OH]	C₁₃H₁₃N₃OS₂Cl₂Cu	Brown	597.5	52.60 (52.21)	4.50 (4.35)	14.30 (14.06)	10.56 (10.63)	–	20
C₄	[Cu(H₂L)₂Cl]·1/2H₂O	C₂₆H₂₇N₆O₂.₉S₂ClCu	Brownish green	626.0	49.70 (49.84)	4.20 (4.31)	13.40 (13.42)	10.05 (10.15)	5.46 (5.67)	14
C₅	[Cu₂(H₂L)₃OH)₂]	C₃₉H₄₁N₉O₅S₃Cu₂	Green	938.1	50.10 (49.90)	4.50 (4.30)	13.50 (13.40)	14.32 (13.50)	–	18

Λ_m = molar conductivity ohm^{-1} cm^2 mol^{-1} in 10^{-3} M DMF.
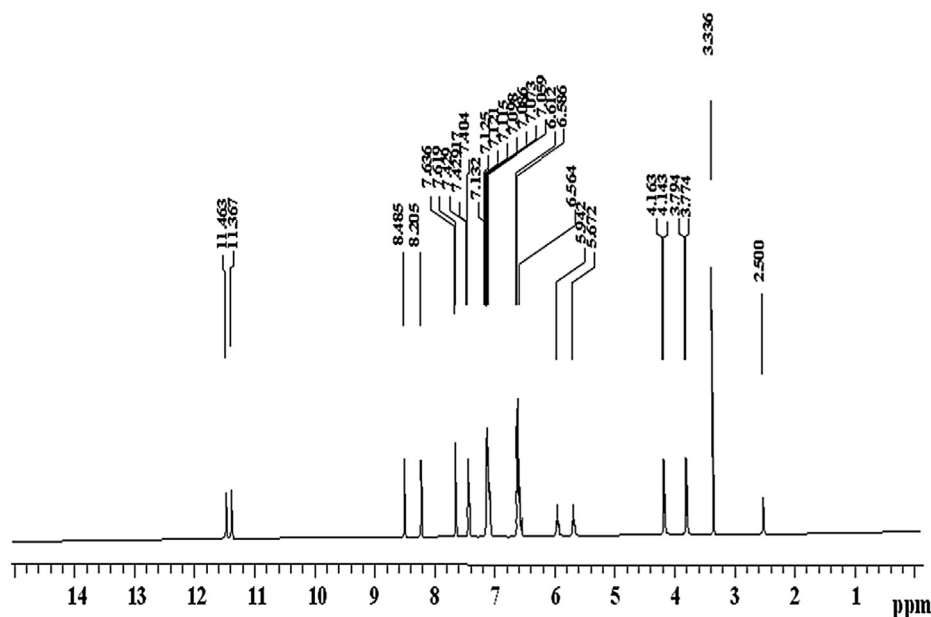
Fig. 1 Proton nuclear magnetic resonance spectrum of (Z)-2-(phenylamino)-N′-(thiophen-2-ylmethylene) acetohydrazide (H₂L).

(2H, —CH=N—), (2H, —CO—NH—) and thiophene ring protons, respectively. Moreover, the spectrum exhibits signals at δ 3.77 ppm due to nonequivalent methylene protons. Thus, the ¹H NMR result supports the assigned of geometry.

The ¹H NMR spectrum of the ligand was verified in DMSO-d_6 solution δ ppm: (Fig. 1). The ¹H NMR spectrum exhibits signal at 2.36 (s, 2H, CH₂), 4.14 (br, 1H, NH), 6.58–7.63 (m, 8H, aromatic system), 5.94 (s,1H, CH), 11.36 (s,1H, NH) (amide α to hydrazone linkage).

3.1.2. ¹³C NMR spectrum of the ligand

The ¹³C NMR spectrum of the ligand (DMSO-d_6) features a signal at 57.5 ppm corresponding to the methylene group. The aromatic carbons of the phenyl ring are observed at 113.5, 120.8, 129.5 and 147.6 ppm (El-Saied et al., 2017) whereas the thiophene ring carbons appear at 127.2, 128.5 and 130 ppm (Nursen and Perihan, 2004; Chandrasekaran et al., 2014). The signal of the azomethine carbon is observed at 125 ppm (Juvansinh et al., 2015). The chemical shift appeared at 171 ppm can be assigned to the carbonyl group (see Fig. 2).

3.1.3. Mass spectrum of the ligand

The electron impact (EI) mass spectrum of the ligand (Fig. 3) confirms the proposed formula, the observed peak at $m/z = 259 amu$ (M) corresponding to the ligand moiety (C₁₃-
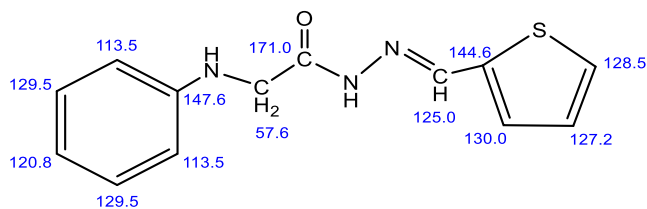
Fig. 2 ¹³C NMR of (Z)-2-(phenylamino)-N′-(thiophen-2-ylmethylene) acetohydrazide.

H₁₃N₃OS, atomic mass $m/z = 259$ molecular ion peak). The series of peaks in the range $m/z = 51$ [C₄H₄-H]⁺, 77 [C₆H₅]⁺, 106 [C₇H₈N]⁺ base peak, 132 [C₈H₈NO-2H]⁺, 149 [C₈H₉N₂O]⁺, may be assigned to different fragments.

3.1.4. Infrared spectra of the ligand and its metal complexes

The IR spectrum of free ligand is compared with IR spectra of its metal complexes, to investigate the mode of bonding Schiff base ligand to metal ion. The characteristic bands of the IR spectrum of the Schiff base ligand are listed in Table 2 and Fig. 4. The broad band at 1628 cm⁻¹ is assigned to the (—C=O, —CH=N) stretching frequency. The IR spectrum of the ligand additionally shows a broad band at 3381, 3244 cm⁻¹ due to the stretching vibration of υ(NH) group (Table 2). On complexation, the IR spectra of all complexes display the bands of the imine groups has shifted to lower wave number as compared of free Schiff base ligand. Also the bands of carbonyl group was shifted to lower wavenumber accompanied by a decrease in their intensity, indicating that they are involved in complex formation (Morsy et al., 2011; Samar, 2017). Complexes (C₃, C₅) showed that the ligand in keto-enolform and enolic oxygen is added to the coordination of complexes (Cescon, 1962; Kumar and Ramesh, 2005; Balasubramanian et al., 2006; Yin and Chen, 2006). The appearance of two new bands at 427–485 and 503–575 cm⁻¹ ranges corresponds to v(M—N) and v(M—O), respectively (Fernandez et al., 2006; Majumder et al., 2006). Complexes (C₁ and C₄) under investigation included water molecules. The broad bands in the 3336–3444 cm⁻¹ region are due to water of crystallization or coordinated of hydroxo group (Fathy and Samar, 2004). From the IR spectral data and the results mentioned above, it is concluded that, the ligand behaved as a neutral bidentate ligand coordinating through the imine nitrogens and the carbonyl groups oxygen in complexes (C₁, C₂). While in complex C₅ the ligand produces binuclear complex.
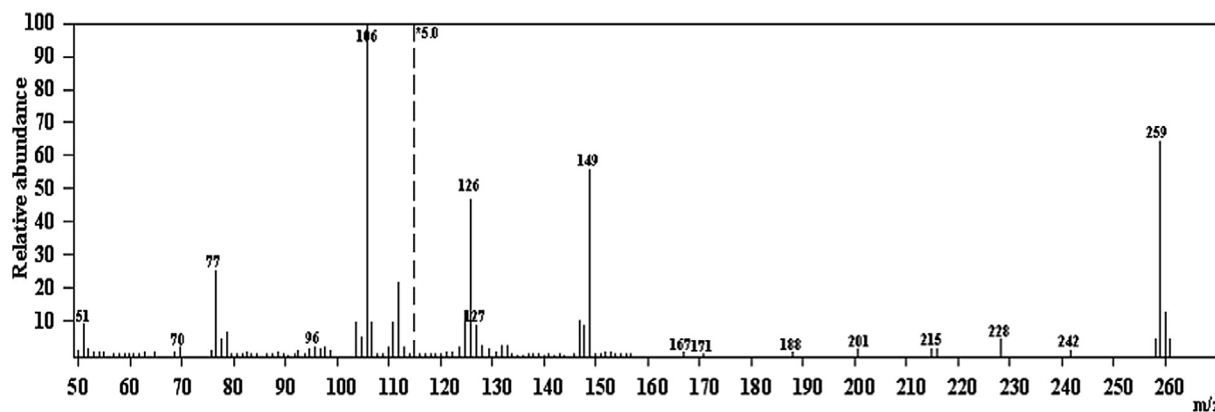
Fig. 3   Mass spectrum of (Z)-2-(phenylamino)-N′-(thiophen-2-ylmethylene)acetohydrazide(H_2L).

Table 2   Infrared spectral bands (cm^{-1}) of ligand and its metal complexes.

NO.	Compound	ν H_2O/OH	ν (N—H)	ν (C=O)	ν (C=N)	ν (C=S)	ν(N—N)	ν (M—N)	ν (M—O)
	H_2L	–	3381,3244	1628	1628	690	1226	–	–
C_1	Pd(H_2L)(OH)Cl]·1/2H_2O	3431	3194,3135	1602	1522	653	1220	438	512
C_2	[Cd(H_2L)Cl$_2$]	3413	3171,3069	**1607**	1595	641	1223	427	503
C_3	[Cu(H_2L)(HL).OH]	3336	3042,3019	1608	1534	690	1220	452	575
C_4	[Cu(H_2L)$_2$Cl]·1/2H_2O	3432	2923	1614	1604	691	1225	455	511
C_5	[Cu$_2$(H_2L)$_3$OH)$_2$]	3444	3336,3091	1606	1534	642	1245	485	571

3.1.5. Electronic spectra and magnetic moments

The electronic spectra of hydrazone ligand and M^{2+}, M^{1+} complexes [where M = Pd(II), Cd (II) and Cu(I, II)] were recorded in 10^{-3} DMF solution in the range 190–800 nm. Within the UV spectrum of the ligand (Table 3) was observed the existence of two absorption bands assigned to the transition π–π* at 250, 325 nm (Table 3). While the electronic spectrum of Pd(II) complex (C_1) displayed bands at 323, 399 and 520 nm, this spin-allowed transition may correspond to $^1A_{1g} \rightarrow {}^1B_{1g}$ transition indicating a square planar geometry (Shankarwar et al., 2015; Hanaa and Ocala, 2015). The electronic spectrum of Cd(II) complex exhibited non-ligand band at 316 nm, referring to L → M charge transfer transition in tetrahedral geometry (Mohamed et al., 2018). Pd(II) and Cd (II) complexes exhibit diamagnetic character (Azam et al., 2012).

Also, The electronic spectra of the copper complexes (C_3-C_5), showed strong absorption bands in the spectra at 325–340 nm attributed to the transition of the ligand between different energy levels. The other band at 379–440 nm is probably assigned to ligand to metal charge transfer (LMCT) transition. One more spectral band appeared at 600–615 for Cu complexes which is due to d-d transitions, which are consistent with the distorted square-pyramidal structure (Li and Xu, 1999; Hathaway et al., 1987). The room temperature magnetic moment value of the Cu complex (C_3) is found to be 1.75B.M. which are close to the spin only value of one unpaired electron. However, the complexes (C_4 and C_5) showed diamagnetic character. The proposed structures are shown in Scheme 2.

3.1.6. Thermal studies of the ligand and its complexes

The thermogravimetric (TG/DTG) analysis is very important technique used to assess the stability of compounds and sup-

port their geometry structure. TG/DTG results of ligand and its complexes (C_1–C_5) are listed in Table 4 and Figs. 5a–5c. The thermal studies of the reported compounds show good agreement with the suggested theoretical formulae obtained from analytical and spectral data (Ahamed et al., 2003).

3.1.6.1. Ligand. The TGA curve of the ligand shows one successive decomposition step within the temperature range 30–320 °C with endothermic DTG peak at 293 °C which assigned to total mass loss parts of ligand (Calc./Found%:100/99.89%).

3.1.6.2. Palladium(II) chelate. The TGA thermoanalytical curves of Pd(II) complex (C_1) shows mass loss (Calc./Found %: 2.11/3.0) with DTG peak at 46 °C, assigned to liberation of half molecule of lattice water within the temperature at 29–103 °C. The thermoanalytical curves also shows one step of decomposition within temperature range 103–799 °C with mass loss of (Calc/Found%:69.22/68.47) associated with DTG peaks at 243, 334, 414 °C leaving metal oxide PdO (Calc./Found%: 28.60/28.28) as final residue (Mishra et al., 2009).

3.1.6.3. Cadmium(II) chelate. The TGA curve of Cd(II) complex (C_2) displays steady part till 192 °C indicating the absence of any outside lattice water or solvent within the temperature range 30–192 °C followed by decomposition step within temperature range 192–799 °C with mass loss (Calc./Found%: 74.69/ 75.50) associated with DTG peaks at 249, 341, 627 °C ended with Cd metal (Calc./Found%: 25.40/24.50) as final thermo product.

3.1.6.4. Copper (II, I) chelates. The TGA thermoanalytical curves of Cu complexes (C_3–C_5) were discussed as follows. The TGA thermogram of Cu(II) complex (C_3) shows steady
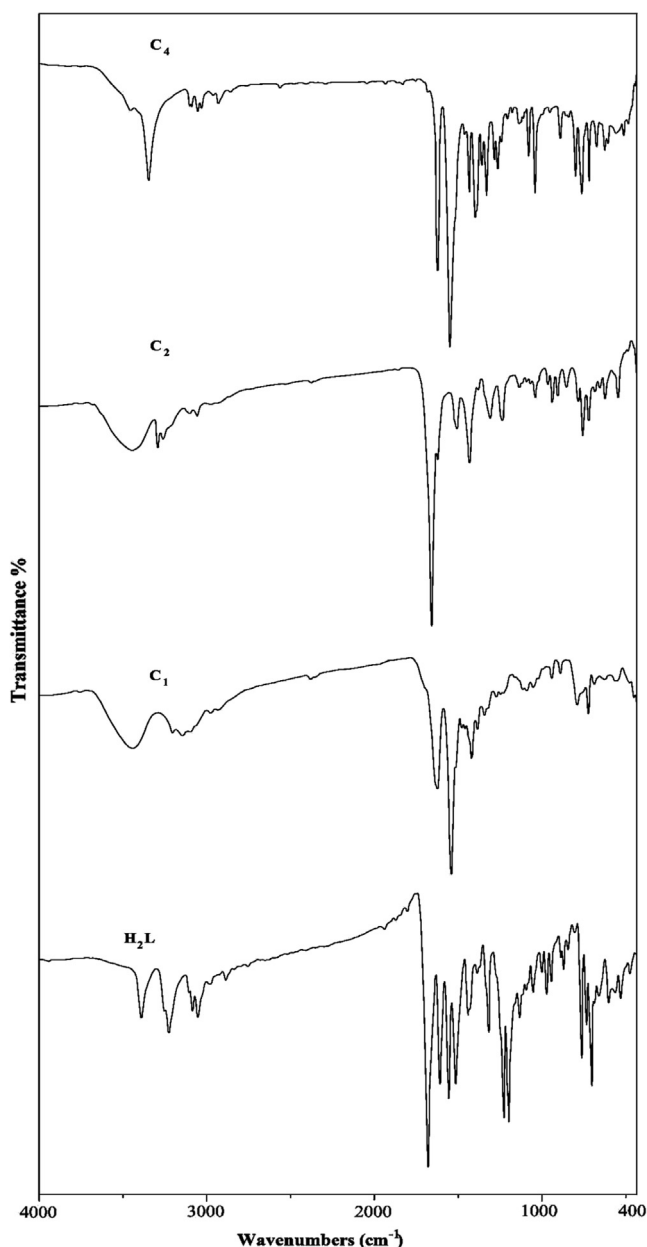
Fig. 4 Infrared spectra of ligand and its metal complexes (C₁, C₂, C₄).
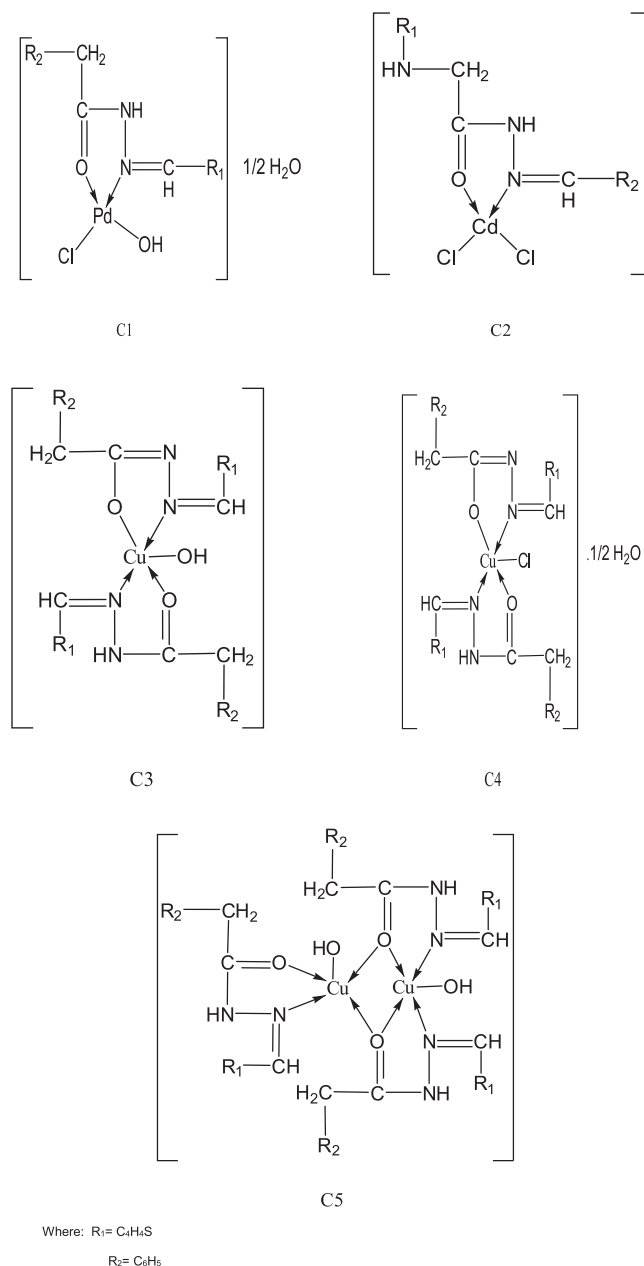
Scheme 2 Suggested chemical structure of Pd(ll), Cd(ll), Cu(l, ll) complexes.

Table 3 Electronic absorption spectra λ_{max}(nm) room temperature effective magnetic moment values μ_{eff}(B.M.) of ligand and its complexes.

No.	Compound	λ_{max}(nm)	μ_{eff}(B.M.)
	H_2L	250, 325	–
C₁	Pd(H_2L)(OH)Cl]·1/2H_2O	323, 399, 520	Dia
C₂	[Cd(H_2L)Cl₂]	316	Dia
C₃	[Cu(H_2L)(HL).OH]	325, 379, 420, 615	1.75
C₄	[Cu(H_2L)₂Cl]·1/2H_2O]	338, 389, 440, 607	Dia
C₅	[Cu₂(H_2L)₃ (OH)₂]	340, 379, 600	Dia

part till 155 °C indicating the absence of any hydrated molecules. The complex decomposes in one step in the temperature range 155–776 °C with mass loss (Calc./Found% 72.64/72.20) associated with DTG peaks at 247, 506, 697, 776 with the production of CuO and carbon residue.

The TGA curve of (C₄) complex displays mass loss (Calc./Found%: 1.44/1.47) within the temperature ranges 33–100 °C with DTG peak at 78 °C which corresponds to loss of half molecule of lattice water. The thermogram also shows more stage of decomposition within temperature range 100–799 °C associated with DTG peaks at 236, 638, 706 °C, according to mass loss (Calc./Found%: 76.28/76.45), respectively, leaving metal oxide contaminated with carbon atoms as residue.

Table 4 DTG and TG data of the ligand and its metal complexes.

No	Compound	Temp. range/°C DTG	Temp. range/°C TGA	Mass loss% Calc. (F)	Reaction	Leaving species
	H_2L	293	30–320	100(99.89)	ii[b]	Decomp.
C_1	$Pd(H_2L)(OH)Cl\cdot 1/2H_2O$	46	29–103	2.11(3.0)	i[a]	$-1/2H_2O$
		243, 334, 414	103–799	69.22 (68.47)	ii[b]	Decomp.
		At799		28.60(28.28)	i[c]	PdO
C2	$[Cd(H_2L)Cl_2]$	249, 341, 627	192–799	74.69(75.50)	ii[b]	Decomp.
		At799		25.40 (24.50)	i[c]	Cd
C_3	$[Cu(H_2L)(HL).OH]$	197, 247, 506	155–776	72.64 (72.20)	ii[b]	Decomp.
		697, 776	At 776	27.36 (27.80)	i[c]	CuO + 7C
C4	$[Cu(H_2L)_2Cl]\cdot 1/2H_2O$	78	33–100	1.44(1.47)	i[a]	$-1/2H_2O$
		236, 638,	100–799	76.28(76.45)	ii[b]	Decomp.
		706	At 799	22.29(22.08)	i[c]	CuO + 5C
C_5	$[Cu_2(H_2L)_3OH)_2]$	197, 697, 776	135–799	73.61(73.50)	ii[b]	Decomp.
			At 799	25.91(26.50)	i[c]	2CuO + 7C

where
i[a] = Dehydration, i[b] = Decompostion, i[c] = Finial residue.
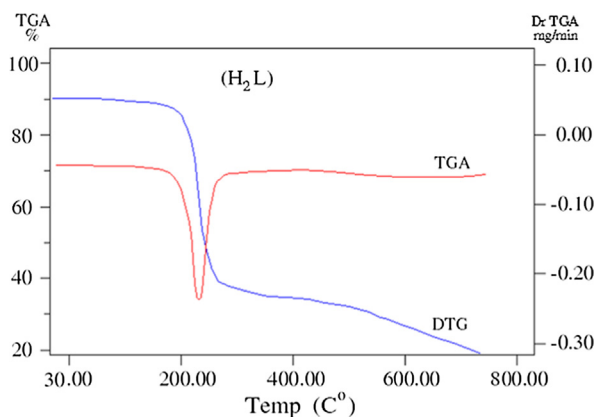
Fig. 5a TG/ DTG curves of the ligand.

Fig. 5b TG/ DTG curve of the Pd(ll) complex (C_1).

Fig. 5c TG/ DTG curve of the Cu(l) complex (C_4).

Moreover, the TGA thermoanalytical curves of (C_5) complex exhibits a steady part till 135 °C, indicating the absence of any outside residual solvent. This step was followed by gradual decomposition within temperature range 135–799 °C associated with DTG peaks at 197, 697, 776 °C, respectively. The decomposition stage ended with the formation of CuO contaminated with carbon atoms as final residue (Calc./Found%: 25.9/26.5), respectively (Harinath et al., 2013). The slight higher value found for the percentage of the residue when compared with the theoretical value for pure metal oxides shows that the residue is contaminated with carbon (Hanaa, 2005).

3.1.7. Kinetic and thermodynamic parameters

The kinetic parameters of activation energy (E), reaction order (n) and the pre-exponential factor (A) were calculated using the Coats–Redfern equation (Coats and Redfern, 1964). As well as the thermodynamic activation parameters for the thermal decomposition steps in complexes; enthalpy (ΔH*), entropy (ΔS*) and free energy of decomposition (ΔG*) were evaluated using the following relationships:

$$\Delta H^* = E^* - RT$$

$$\Delta S^* = R[\ln(Ah/kT) - 1]$$

$$\Delta G^* = \Delta H^* - T\Delta S^*$$

where k is Boltzmann constant and h is Plank's constant and R is the gas constant. The kinetic parameters obtained from the

previously mentioned methods are listed in Table 5 and Figs. 6a–6d.

From the results, the following remarks can be pointed out:

- The positive sign of ΔG* for the complexes under investigation revealed that the free energy of the final residue is higher than that of the initial compound and all the decomposition steps are non-spontaneous processes.
- The negative values of ΔS* for the degradation process indicated a more order activated complex than reactant and/or the reaction was slow (Frost and Pearson, 1961).
- All the complexes have negative entropy, which indicates that the complexes are formed spontaneously.
- The positive values of ΔH* means that the decomposition processes were endothermic (El-Ayaan et al., 2007).
- Kinetics of the thermal decomposition stages of the complexes under study obeys, in most cases, the first order kinetics.
- The values of ΔG* increased for the subsequent decomposition stage of complex C_1. This increase in the values of ΔG* reflected that the rate of removal of the subsequent ligand was lower than that of the precedent ligand, this is due to increasing in the values of TΔS* from one step to another which overrides the values of ΔH* (Maravalli and Goudar, 1978; Yusuff and Sreekala, 1990; Vinodkumar et al., 2000).
- It was found that the order of the activation energy values of the first decomposition step for the complexes is: $C_3 > C_5 > C_4 > C_1 > C_2$.

3.1.8. X-ray diffraction

XRD pattern of copper complex (C_4) is revealed in Table 6 and Fig. 7. The X-ray powder diffraction analysis of (C_4) complex was carried out to give information about atomic or molecular arrangement as shown in Fig. 7. The spectra showed sharp peaks indicating their crystalline nature. The X-ray powder diffraction patterns were attained in the range of 5–90° and in steps of 0.050°. The full width at the half- maximum (FWHM) of diffraction peaks observed from the refinement was used to evaluate the particle size. Also, to investigate the crystalline information about complex, the average crystallite
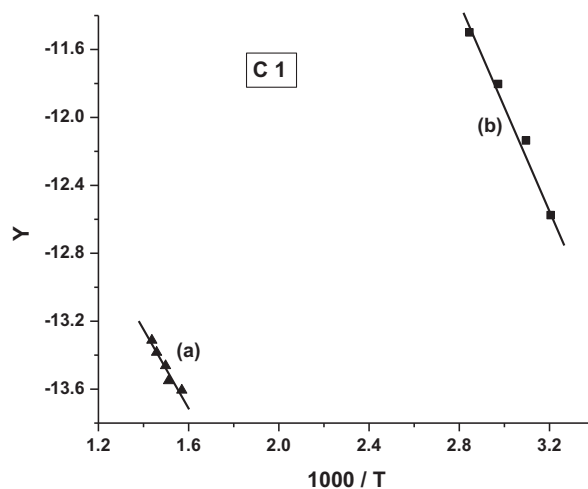
Fig. 6a Coats-Redfern plot for complex C_1.
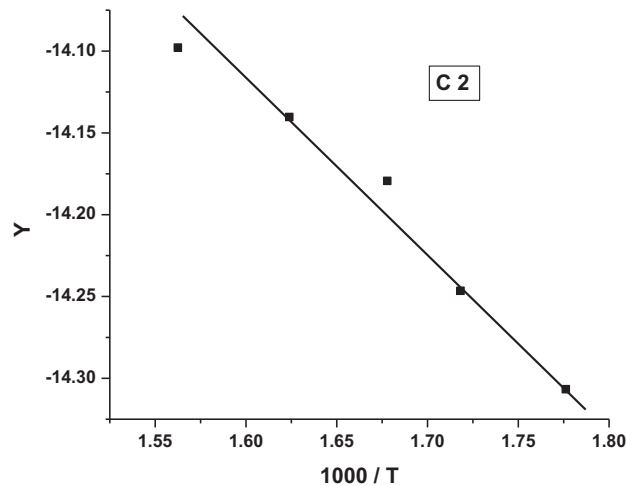
Fig. 6b Coats-Redfern plot for complex C_2.

Table 5 Temperature of decomposition and activation parameters (ΔH*, ΔS*, ΔG*) for decomposition of complexes using Coats-Redfern (CR).

Complex	n	Step	r	T (K)	E*	ΔH*	A	−ΔS*	Δ G*
C_1	1	1st	0.9926	330.75	24.476	21.730	643661.330	0.1429	68.910
	0	2nd	0.9672	669.62	18.694	13.132	548491248.3	0.0926	75.109
C_2	0.66	1st	0.9865	599.36	8.273	3.293	2,753,329,374	0.0783	50.200
C_3	1	2nd	0.9938	511.16	95.953	91.705	18.7038612	0.2333	210.948
C_4	1	1st	0.9989	344.57	40.332	37.468	9819.302904	0.1780	98.789
	0.5	2nd	0.9993	606.30	10.498	5.459	1,029,166,719	0.0866	57.931
C_5	1	1st	0.9825	482.88	47.452	43.437	550951.946	0.1473	114.596

Where:
E: the activation energy (KJ.mol^{-1}), ΔH*: the activation enthalpy (KJ.mol^{-1}),
ΔS*: the entropy (J.K^{-1}.mol^{-1}), A: the pre-exponential factor (s^{-1}),
ΔG*: the free energy (KJ.mol^{-1}).
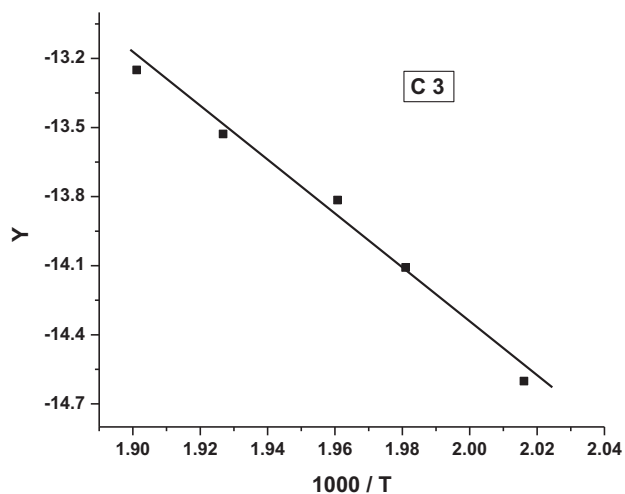
Fig. 6c Coats-Redfern plot for complex C_3.
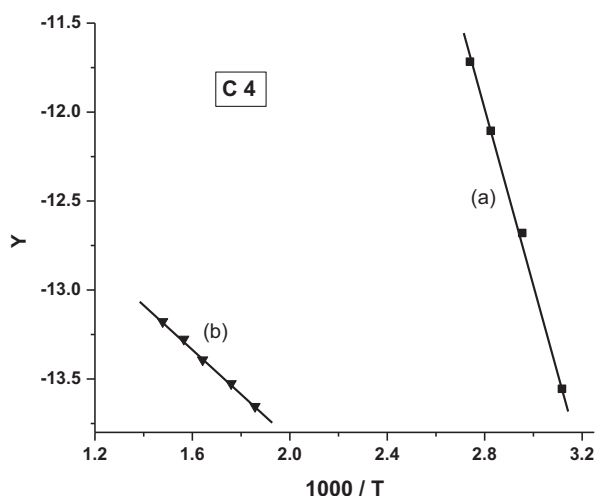
Fig. 6d Coats-Redfern plot for complex C_4.

sizes (D) were calculated from the most sharp peaks using Sherrer's formula (Harikumaran and Appukuttan, 2012).

$$D = (K\lambda/\beta Cos\theta)$$

The diffraction peaks indicate that synthesized of copper complex (C_4) is in the nanometer range. Also, the average crystallite size of C_4 complex is 4.107 nm. From the value of (D), we can obtain the dislocation density (δ) value of complex which indicates the number of dislocation lines per unit area of the crystal. The value of (δ) is related to the average crystallite size (D) from the equation:

$$\delta = 1/(D)^2$$

The calculated value of (δ) found to be 0.0593.

3.1.9. Molecular modeling

Many attempts to prepare crystals for X-ray crystallography were unsuccessful. The computational strategy in this manuscript is to determine the geometry of the ligand and its complex. Thus, molecular modeling calculations were considered. Thus, the geometries of the complexes were optimized by hyper chem. 8.03 Molecular Modeling and Analysis Program using the molecular mechanics calculations (PM3) (HyperChem, 2007).

The optimized geometries of the ligand and its complexes are shown in Figs. 8a–8c. The optimized lengths of bonds in addition to bond angles (Supplementary materials) are listed in Tables (S_1-S_3). The energetic properties of these compounds are listed in Table 8.

From selected bond lengths collected in Table 7 one can conclude the following remarks:

- In all complexes the metal ions are coordinated to the ligand via N9 and O14 atoms.
- A large variation in C6=N7 and N7—N9 bonds length on coordination via the N7 atom.
- The C6=N7 bond length increases in all complexes than ligand.
- In Pd complex the bond distance N7—N9 is enlarged due to their participation in coordination which becomes weaker due to the formation of Pd—N bonds (El-Gammal et al., 2014) M—N bond of Cd complex is larger than Pd complex.
- In general, the M—Cl bond length is longer than that of M—N and M—O bonds.
- The bond angles of the ligand moiety are altered somewhat upon coordination (Mohamed et al., 2014).
- The other bond lengths and bond angles also suffer some changes, but not significantly.

Table 6 XRD data for copper complex (C_4).					
Compounds	Peak	^{0}2Th	d-sp	β-FWHM	D(nm)
C_4[Cu(H_2L)$_2$Cl]·1/2H_2O]	1	7.97	11.0838	0.2887	4.81
	2	11.49	7.6963	0.3286.6	4.24
	3	13.13	6.7385	0.3059	4.56
	4	16.23	5.4561	0.3577	3.90
	5	16.87	5.2519	0.2602	5.38
	6	20.71	4.2849	0.2827	4.98
	7	21.51	4.1270	0.2126	6.64
	8	22.28	3.9872	0.4925	2.86
	9	27.24	3.2714	0.2814	5.07
	10	3235	2.7653	0.5139	2.74
Mean of D					4.107
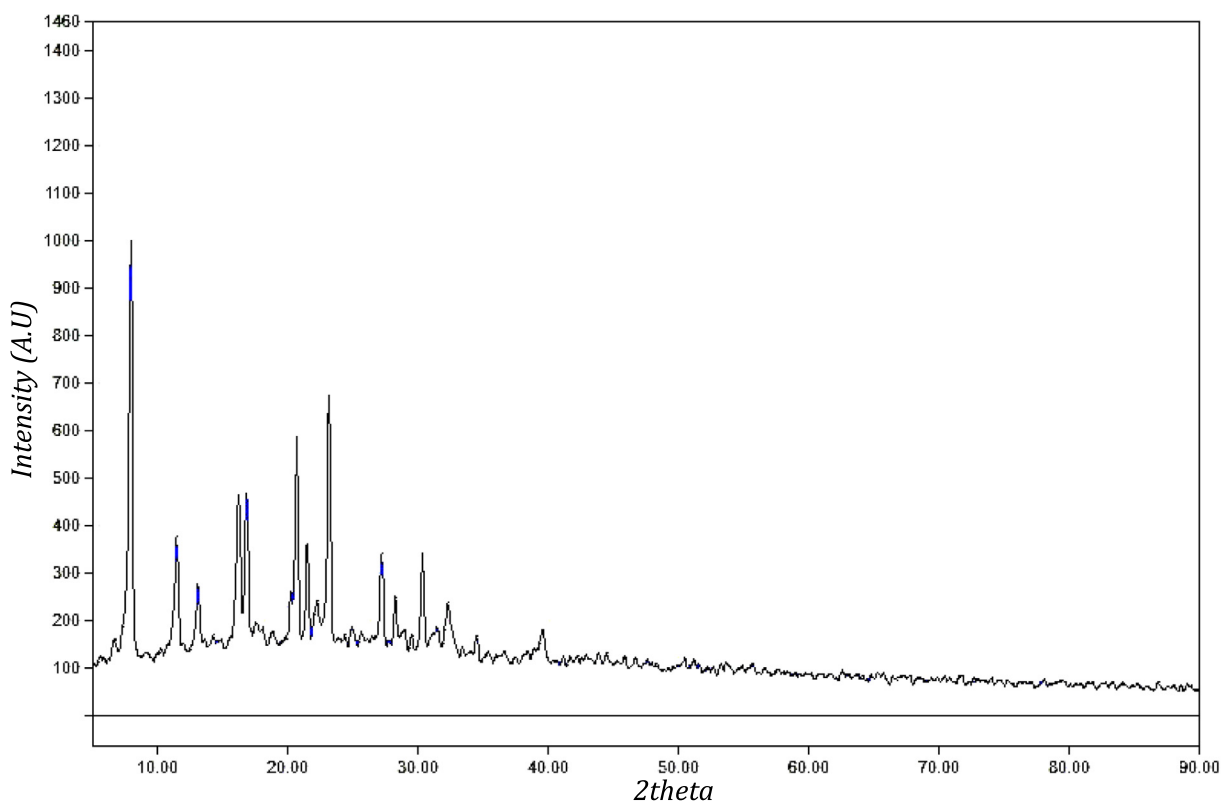
Fig. 7 X-ray diffraction pattern of C$_4$ complex.
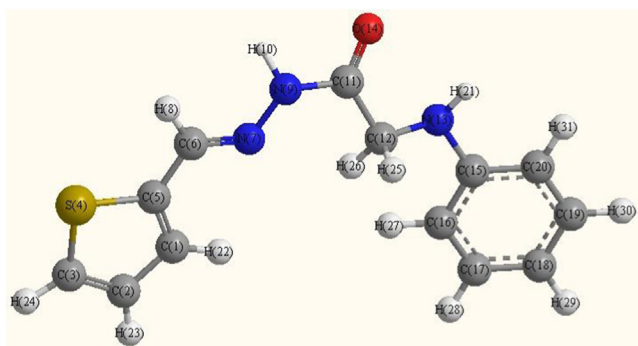
Fig. 8a Optimized molecular structure of ligand.
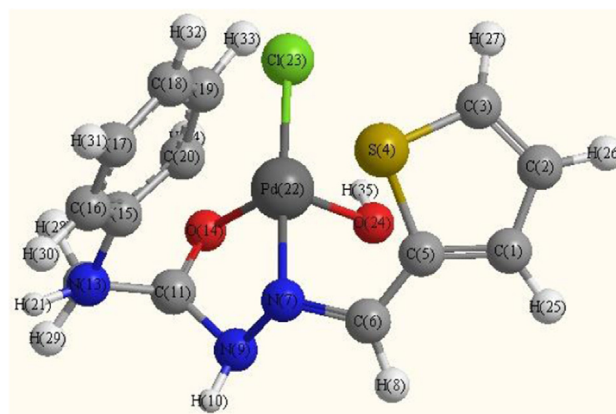
Fig. 8b Optimized molecular structure of Pd(II) complex (C$_1$).

- The bond angles in Pd(II) complex are quite near to a square planer, and tetrahedral geometry in Cd(II) predicting dsp^2 hybridization. The bond angle values show a large distortion around the metal centers.
- The HOMO and LUMO namely the Frontier Molecular Orbitals (FMOs) are very popular quantum chemical parameters. The chemical reactivity is a function of interaction between HOMO and LUMO levels of the reacting species (Kenichi, 1982). The higher E$_{HOMO}$ implies that the molecule is a good electron donor and has great ability to complex formation. LUMO energy presents the ability of a molecule receiving electron (Geerlings et al., 2003; Seda et al., 2009). The lower E$_{LUMO}$ value, the more ability of the molecule is to accept electrons (Guo and Chengha, 2007).

3.2. Biological applications

3.2.1. In vitro antibacterial activity

The antibacterial activities of ligand H$_2$L as well as its metal complexes (C$_1$- C$_5$) were tested against *S. pyogenes* as Gram-positive bacteria and *E. coli* as Gram–negative bacteria. According to the data depicted in Figs. 9 and 10, the following results are summarize as follow:

1-All of the tested compounds are found to have remarkable antibacterial activity. The active sequence of the ligand and its tested complexes against *S. pyogenes* in the concentration of 1 μg/mL, 5 μg/mL follows the trend: C$_1$ > C$_2$ > C$_3$ > C$_5$ > C$_4$ > H$_2$L.
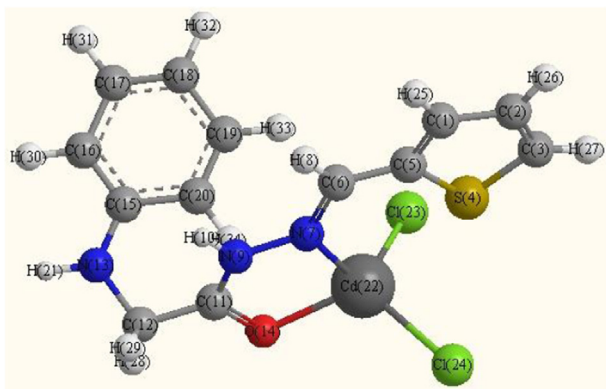
Fig. 8c Optimized molecular structure of Cd(II)complex (C$_2$).

2- Also all the tested complexes except C$_4$, have higher activity than their metal free ligand against *E. coli* for concentration of 1 μg/mL as the follow trend: C$_2$ > C$_3$ > C$_5$ > C$_1$ > H$_2$-L > C$_4$, and for the concentration of 5 μg/mL, the activity follows the trend: C$_2$ > C$_3$ > C$_5$ > C$_1$ > H$_2$L, C$_4$.

3- It is found that, C$_1$ complex has the highest toxicity against Gram-positive bacteria in both two concentrations; C$_2$ has the highest toxicity against gram-negative bacteria in both concentrations. Moreover, it is found that all tested complexes are more toxic against both Gram-positive and Gram-negative bacteria than that of the free ligand in the both concentrations, except C$_4$ in gram-negative bacteria, having higher antibacterial activities than that of the free ligand. This would suggest that, chelation/complexation could enhance the lipophilic character of the central metal atom, which subsequently favors its permeation through the lipid layers of the cell membrane and blocking the metal binding sites on enzymes of

microorganism which as explained by Tweedy's chelation theory (Tweedy, 1964). It is suspected that other factors such as liposolubility, dipole moment, conductivity influenced by metal ion, geometry, number and type of metal ions and counter ions, and moieties as azomethine linkage present in these compounds may be possible reasons for their remarkable antibacterial activities (Mehmet et al., 2010; Dharmpal et al., 2017; Saeed et al., 2009; Najma et al., 2010).

3.2.2. Antioxidant activity

The process of scavenging DPPH-free radicals has been used to assess the antioxidant activity of the present compounds (Bilgicli et al., 2015). The data of the suppression ratio for DPPH are shown in Fig. 11. The results were compared with those of standard antioxidants. The percentage radical scavenging activity of the synthesized compounds has been carried out at different concentrations (100, 200 and 300 μg mL^{-1}). The DPPH scavenging activity was expressed as IC$_{50}$, the effective concentration at which 50% of the radicals were scavenged, have been calculated to assess the antioxidant activities. A lower IC$_{50}$ value indicates greater antioxidant activity. IC$_{50}$ values lower than 10 mg/mL usually imply effective activities in antioxidant properties. Fig. 11 shows that, all of the tested compounds exhibited very good radical scavenging activities at different concentrations. From the obtained results, C$_3$,C$_4$ complexes (IC$_{50}$ = 0.019, 0.211 μg mL^{-1}) showed good activity better all tested compounds and the positive standard. The ligand (IC$_{50}$ = 0.514 μg mL^{-1}) possesses the lowest scavenging ability as compared to the positive standard and all tested complexes. The order of IC$_{50}$ values of ligand and its metal (II,I) complexes was as follows: C$_3$ > C$_4$ > C$_1$ > C$_2$ > Ligand. The free radical scavenging activity of the compounds depends on the structural factors and other structural features as type and geometry of metal ions.

Table 7 The selected bond length (Å) of the ligand and its complexes.

Compound	Bond length									
	C5—C6	C6=N7	N7—N9	N9—C11	C11—C12	C11—O14	C12—N13	N13—C15	M—N	M—O
Ligand	1.4443	1.3093	1.3857	1.4450	1.5130	1.2188	1.4840	1.4380	—	—
C$_2$	1.4428	1.3135	1.3731	1.4564	1.5271	1.2144	1.4822	1.4461	2.2087	2.1872
C$_1$	1.3996	1.4041	1.4872	1.4570	1.5034	1.3338	1.4868	1.4366	1.9674	2.0006
										1.9784

Table 8 The energetic properties of the ligands and its complexes.

The assignment of the theoretical parameters	Ligand	C$_2$	C$_1$
Total energy*	−2980.14	−3108.34	−3755.85
Kinetic Energy*	145.37	198.75	13.70
Binding energy*	−3125.511	−3307.10	−3769.552
Potential energy*	−62198.038	−77434.766	−100987.210
Isolated Atomic Energy*	−59072.527	−74127.670	−97217.658
Electronic Energy*	−385803.42	−450035.21	−679902.63
Core-Core Interaction*	323605.38	372600.45	578915.42
Heat of Formation	238.344	141.46	−175.046
Dipole moment (Debye)	2.195	6.121	6.221
HOMO (eV)	−8.976991	−8.948892	−7.934258
LUMO (eV)	−0.732292	−0.975450	−0.741812
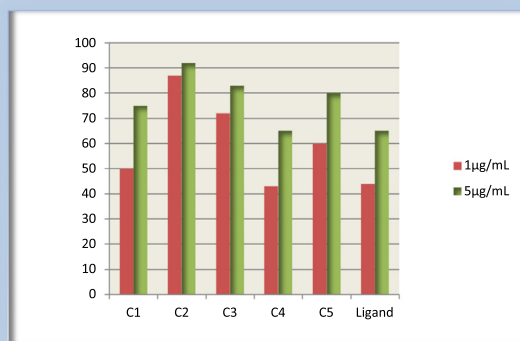
Fig. 9 Antibacterial activity for the ligand and its metal complexes against *E. coli.*
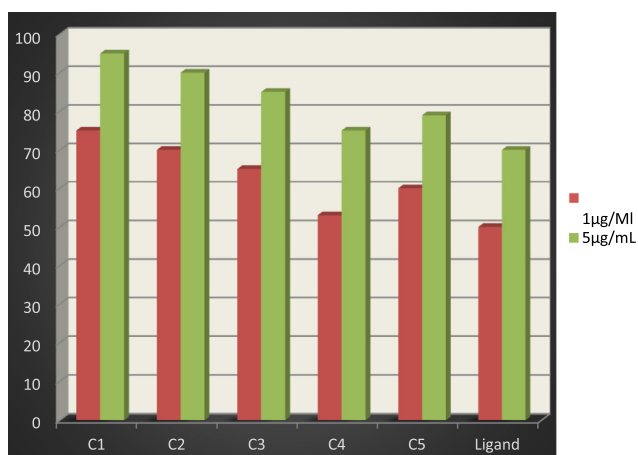
Fig. 10 Antibacterial activity for the ligand and its metal complexes against *S. pyogenes.*
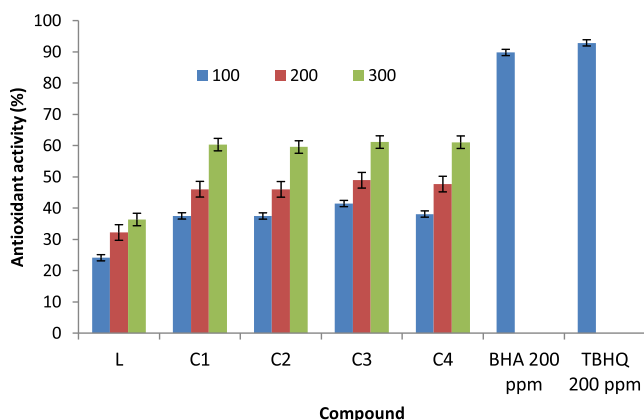
Fig. 11 Antioxidant activity of ligand and its complexes (C$_1$-C$_4$) as determined by DPPH.

4. Conclusions

In this summary, Pd(II), Cd(II) and Cu(I, II) complexes of 2-phenylamino-N-(thiophene-2yl) methylene)acetohydrazide ligand(H$_2$L) have been studied. The analytical and physical techniques recommended the chemical structure of the new complexes. The biological applications such as antibacterial activity and antioxidant of ligand and its complexes are reported. The results found can be summarized as follows:

1. The ligand behaves as neutral bidentate or tetradentate
2. Pd(II) complex (**C$_1$**) is square planar and Cu(II, I) complexes (**C$_3$-C$_4$**) are square pyramidal in geometry. While Cd(II) complex (**C$_2$**) has tetrahedral geometry.
3. X-ray diffraction pattern prove that the crystallite size of the copper complex (**C$_4$**).
4. The computational calculations showed that metal complexes **C$_1$** exhibit square planer and **C$_2$** is tetrahedral geometrical arrangement which agrees well with the experimental observation.
5. In vitro biological applications showed the effective antibacterial and antioxidant activities of the tested compounds. The antibacterial and antioxidant activities of these compounds increase with their coordination.
6. In addition to the complex of copper (**C$_3$**) is more greater antioxidant than all tested compounds.

Declaration of Competing Interest

The authors declare that they have no known competing financial interests or personal relationships that could have appeared to influence the work reported in this paper.

Appendix A. Supplementary material

Supplementary data to this article can be found online at https://doi.org/10.1016/j.arabjc.2019.12.003.

References

Abdel-Aal, M.T., El-Sayed, W.A., El-Ashry, S.H., 2006. Synthesis and antiviral evaluation of some sugar arylglycinoylhydrazones and their oxadiazoline derivatives. Arch. Pharm. Chem. Life Sci. 339, 656–663. https://doi.org/10.1002/ardp.200600100.

Abdülmelik, A., Ercan, B., Fikret, T., Hatice, T., Ömer, K., İlhami, G., Ekrem, K., 2019. Phytochemical content, antidiabetic, anticholinergic, and antioxidant activities of endemic lecokia cretica extracts e1900341 Chem. Biodiversity 16. https://doi.org/10.1002/cbdv.201900341.

Adriana, G., Ovidiu, B., Loredana, B., Thomas, C., Ioana, B., Bruno, T., 2015. Synthesis, anticancer activity, and genome profiling of thiazolo arene ruthenium complexes. J. Med. Chem. 58, 8475–8490. https://doi.org/10.1021/acs.jmedchem.5b00855.

Ahamed, M.D., Hanaa, A.E., Mohamed, F.E., 2003. Thermal investigation of iron(III) and manganese(II, III) complexes of dianils derived from 6-formylkhellin. J. Therm. Anal Calorim. 73, 987–1000. https://doi.org/10.1023/A:10258757494.

Ak, T., Gülçin, I., 2008. Antioxidant and radical scavenging properties of curcumin. Chem. Biol. Interact. 174, 27–37. https://doi.org/10.1016/j.cbi.2008.05.003.

Angel, A.R., Jeferson, G.S., Pryscila, R.C., Raquel, G.S., Heloisa, B., 2014. ROS-mediated cytotoxic effect of copper(II) hydrazone complexes against human glioma cells. Molecules 19, 17202–17220. https://doi.org/10.3390/molecules191117202.

Azam, E.S., EL Husseiny, A.F., Al-Amri, H.M., 2012. Synthesis and photoluminescent properties of a Schiff-base ligand and its mononuclear Zn(II), Cd(II), Cu(II), Ni(II) and Pd(II) metal complexes. Arabian J. Chem. 5 (1), 45–53. https://doi.org/10.1016/j.arabjc.2010.07.022.

Balasubramanian, K.P., Parameswari, K., Chinnusamy, V., Prabhakaran, R., Natarajan, K., 2006. Synthesis, characterization, electro chemistry, catalytic and biological activities of ruthenium (III) complexes with bidentate N, O/S donor ligands. Spectrochim. Acta, Part A 65, 678–683. https://doi.org/10.1016/j.saa.2005.12.029.

Bakr, F., Hassan, G., Ghada, A., Farid, A.B., 2012. Synthesis, antimicrobial, antioxidant, anti-inflammatory, and analgesic activities of some new 3-(20 -thienyl)pyrazole-based heterocycles. Med. Chem. Res. 21, 1418–1426. https://doi.org/10.1007/s00044-011-9661-x.

Bassett, J., Denney, R.C., Jeffery, G.H., Mendham, J., 1978. Vogel's Textbook of Quantitative Inorganic Analysis Including Elementary Instrumental Analysis. Longman Group, London, p. 316.

Bayoumi, H.A., Alaghaz, A.M., Aljahdali, M.S., 2013. Cu(II), Ni(II), Co(II) and Cr(III) complexes with N2O2-chelating Schiff's base ligand incorporating Azo and sulfonamide moieties: spectroscopic, electrochemical behavior and thermal decomposition studies. Int. J. Electrochem. Sci. 8, 9399–9413. www.electrochemsci.org.

Bijev, A., 2006. New heterocyclic hydrazones in the search for antitubercular agents: synthesis and in vitro evaluations. Lett. Drug Des. Discov. 3, 506–512. https://doi.org/10.2174/157018006778194790.

Bilgicli, A.T., Tekin, Y., Alici, E.H., Yaraşir, M.N., Arabaci, G., Kandaz, M., 2015. J. Coord. Chem. 68, 4102. https://doi.org/10.1080/00958972.2015.1080361.

Blois, M.S., 1958. Antioxidant determinations by the use of a stable free radical. Nature 181, 1199–1200.

Cescon, L.A., 1962. Day, A.R., Preparation of some benzimidazolylamino acids. Reactions of amino acids with o-phenylenediamines. J. Org. Chem. 27 (2), 581–586. https://doi.org/10.1021/jo01049a056.

Chavarria, G.E., Horsman, M.R., Arispe, W.M., Kumar, G.D.K., Chen, S.E., Strecker, T.E., Parker, E.N., Chaplin, D.J., Pinney, K. G., Trawick, M.L., 2012. Initial evaluation of the antitumour activity of KGP94, a functionalized benzophenone thiosemicarbazone inhibitor of cathepsin L. Eur. J. Med. Chem. 58, 568–572. 10.1016/j.ejmech.2012.10.039.

Chandrasekaran, T., Suresh, M., Ahamed, F.M., Padusha, M., 2014. Synthesis, characterization and antimicrobial studies of novel compound and its metal complexes derived from nicotinic acid. Der Chemica Sinica 5 (5), 81–90. www.pelagiaresearchlibrary.com.

Coats, A.W., Redfern, J.P., 1964. Kinetic parameters from thermogravimetric data. Nature 201, 68–69. https://doi.org/10.1038/201068a0.

Daniela, S., Simone, C., Anél, P., Paolo, G., Melissa, D., Paola, C., Donatella, B., Stefano, A., Gokhan, Z., Jacobus, P., Francesco, O., 2019. 4-(3-Nitrophenyl)thiazol-2-ylhydrazone derivatives as antioxidants and selective hMAO-B inhibitors:synthesis, biological activity and computational analysis. J. Enzyme Inhib. Med. Chem. 34, 597–612. https://doi.org/10.1080/14756366.2019.1571272.

Dharmpal, P.S., Vidhi, G., Parveen, R., Kiran, J., 2017. Trivalent transition metal complexes derived from carbohydrazide and dimedone. Arab. J. Chem. 10, S1795–S1801. https://doi.org/10.1016/j.arabjc.2013.07.004.

Dominik, A.M., Kristin, R., Christian, R., Jutta, K., Barbara, S., Jens, M., 2017. Structurally related hydrazone-based metal complexes with different antitumor activities variably induce apoptotic cell death. Dalton Trans. 46, 4759–4767. https://doi.org/10.1039/c6dt04613.

El-Saied, F.A., Al-Hakimi, A.N., Wahba, M.A., Shakdofa, M.M.E., 2017. Preparation, characterization and antimicrobial activities of N'-((3-(hydroxyimino) butan-2-ylidene)-2 (phenylamino) acetohydrazide and its metal complexes. Egypt. J. Chem. 60 (1), 1–24. https://doi.org/10.21608/ejchem.2017.620.1010.

El-Sharief, M.A., Abbas, S.Y., El-Bayouki, K.A., El-Gammal, E.W., 2013. Synthesis of thiosemicarbazones derived from N-(4-hippuric acid)thiosemicarbazide and different carbonyl compounds as antimicrobial agents. Eur. J. Med. Chem. 67, 263–268. https://doi.org/10.1016/j.ejmech.2013.06.031.

El-Ayaan, U., Kenawy, I., Abu El-Reash, Y., 2007. Synthesis, thermal and spectral. Studies of first-row transition metal complexes with Girard-T reagent-based ligand. Spectrochim. Acta, Part A 68, 211–219. https://doi.org/10.1016/j.saa.2006.11.016.

El-Gammal, O.A., Abu El-Reash, G.M., El-Gamil, M.M., 2014. Synthesis, characterization, DFT and biological studies of isatin-picolinohydrazone and its Zn(II), Cd(II) and Hg(II) complexes. Spectrochim. Acta, Part A 127, 144–156. https://doi.org/10.1016/j.saa.2014.02.008.

Ercan, B., Ilhami, G., 2011. Polyphenol contents and in vitro antioxidant activities of lyophilised aqueous extract of kiwifruit (Actinidia deliciosa). Food Res. Int. 44, 1482–1489. https://doi.org/10.1016/j.foodres.2011.03.031.

Fathy, A.E., Samar, A.A., 2004. Synthesis and characterization of UO2(VI), Sn (IV), and Th (IV) complexes of 4-formylazohydrazoaniline antipyrine. Afinidad 61 (514), 516–520.

Ferreira, I.P., Piló, E.D.L., Recio-Despaigne, A.A., Da Silva, J.G., Ramos, J.P., Marques, L.B., Prazeres, P.H.D.M., Takahashi, J.A., Souza-Fagundes, E.M., Rocha, W., Beraldo, H., 2016. Bismuth (III) complexes with 2-acetylpyridine- and 2-benzoylpyridine-derived hydrazones: Antimicrobial and cytotoxic activities and effects on the clonogenic survival of human solid tumor cells. Bioorg. & Med. Chem. 24, 2988–2998. https://doi.org/10.1016/j.bmc.2016.05.007.

Fernandez, G.M., Tepal-Sanchez, P., Hernandez-Ortega, S., 2006. The crystal structures of some -o-hydroxy Schiff base copper(II) complexes derived from (R) and (S) secbutylamines. J. Mol. Struct. 787, 1–7. https://doi.org/10.1016/j.molstruc.2005.10.023.

Frost, A.A., Pearson, R.G., 1961. Kinetics and Mechanisms. Wiley, New-York. https://doi.org/10.1021/ed038p535.1.

Geerlings, P., De Proft, F., Langenaeker, W., 2003. Conceptual density functional theory. Chem. Rev. 103, 1793–1874. https://doi.org/10.1021/cr990029p.

Guo, G., Chengha, L., 2007. Electrochemical and DFT studies of β-amino-alcohols as corrosion inhibitors for brass. Electro Chim. Acta 52, 4554–4559. https://doi.org/10.1016/j.electacta.2006.12.058.

Gülçin, I., Bursal, E., Sehitoğlu, M.H., Bilsel, M., Gören, A.C., 2010. Polyphenol contents and antioxidant activity of lyophilized aqueous extract of propolis from Erzurum, Turkey. Food Chem. Toxicol. 48, 2227–2238. https://doi.org/10.1016/j.fct.2010.05.053.

Gülçin, I., 2006a. Antioxidant and antiradical activities of L-carnitine. Life Sci. 78, 803–811. https://doi.org/10.1016/j.lfs.2005.05.103.

Gülçin, I., 2006b. Antioxidant activity of caffeic acid (3,4-dihydroxycinnamic acid). Toxicol. 217, 213–220. https://doi.org/10.1016/j.tox.2005.09.011.

Hanaa, A.E., 2005. Structural and thermal studies of some aroylhydrazone Schiff's bases-transition metal complexes. J. Therm. Anal. Calorim. 81, 339–346. https://doi.org/10.1007/s10973-005-0789-0.

Hanaa, A.E., Ocala, A., 2015. New 15-membered tetraaza (N4) macrocyclic ligand and its transition metal complexes: spectral, magnetic, thermal and anticancer activity. Spectrochim. Acta A 138, 553–562. https://doi.org/10.1016/j.saa.2014.11.015.

Harinath, Y., Reddy, D.K., Kumar, B.N., Apparao, C., Seshaiah, K., 2013. Synthesis, spectral characterization and antioxidant activity studies of a bidentate Schiff base, 5-methyl thiophene-2-carbox-

aldehyde-carbohydrazone and its Cd(II), Cu(II), Ni(II) and Zn(II) complexes. Spectrochim. Acta A 101, 264–272. https://doi.org/10.1016/j.saa.2012.09.085.

Hasnah, O., Afsheen, A., Chan, K.L., Mark, C.B., 2012. Microwave-assisted synthesis and antioxidant properties of hydrazinyl thiazolyl coumarin derivatives. Chem. Cent. J. 6 (32), 1–10. https://doi.org/10.1186/1752-153X-6-32.

Hathaway, B.J., Wilkinson, G., Gillard, R.D., McCleverty, J.A., (Eds.) 1987. New York: Pergamon, 6, pp. 317–410.

Harikumaran, M.L., Appukuttan, A.S., 2012. Syntheses, spectral, surface morphological and gamma ray irradiation studies of some oxomolybdenum(V) and dioxomolybdenum(VI) complexes of an azo dye derived from 4-aminoantipyrine. J. Korean Chem. Soc. 56, 217–227. https://doi.org/10.5012/jkcs.2012.56.2.217.

HyperChem, 2007. Release 8.03 for Windows, Molecular Modeling System, Hypercube Inc.

Ibrahim, H., Abou-seri, S., Ismail, N., Elaasser, M., Aly, M., Abdel-Aziz, H., 2016. Bis-isatin hydrazones with novel linkers: Synthesis and biological evaluation as cytotoxic agents. Eur. J. Med. Chem. 108, 415–422. https://doi.org/10.1016/j.ejmech.2015.11.047.

Imramovsky, A., Polanc, S., Vinsova, J., Kocevar, M., Jampitek, J., Reckova, Z., Kaustova, J.A., 2007. A new modification of anti-tubercular active molecules. Bioorg. Med. Chem. Lett. 15, 2551–2559. https://doi.org/10.1016/j.bmc.2007.01.051.

Jaishree, V., Ramdas, N., Sachin, J., Ramesh, B., 2012. In vitro antioxidant properties of new thiazole derivatives. J. Saudi Chem. Soc. 16, 371–376. https://doi.org/10.1016/j.jscs.2011.02.007.

Jiayang, J., Yuanyuan, Q., Zihan, X., Zhuang, L., Peng, T., Mingjuan, X., Shujuan, L., Wei, H., Qiang, Z., 2019. Enhancing singlet oxygen generation in semiconducting polymer nanoparticles through fluorescence resonance energy transfer for tumor treatment. Chem. Sci. 10, 5085–5094. https://doi.org/10.1039/C8SC05501G.

Juvansinh, J., Mayank, M., Mitesh, G., Rohit, M., Manish, R., Shah, M.K., 2015. Synthesis, spectral analysis and evolution of antimicrobial activity of Schiff base of cyanoacetohydrazide. Int. Lett. Chem., Phys. Astron. 52, 100–110. http://doi.10.18052/www.sci-press.com/ILCPA.52.100.

Kaan, K., Halise, I., Parham, T., Ilhami, G., Claudiu, T., 2019. Investigation of inhibitory properties of some hydrazone compounds on hCA I, hCA II and AChE enzymes. Bioorg. Chem. 86, 316–321. https://doi.org/10.1016/j.bioorg.2019.02.008.

Kesel, A.J., 2011. Broad-spectrum antiviral activity including human immunodeficiency and hepatitis C viruses mediated by a novel retinoid thiosemicarbazone derivative. Eur. J. Med. Chem. 46, 1656.-1664. https://doi.org/10.1016/j.ejmech.2011.02.014.

Kenichi, F., 1982. Role of frontier orbitals in chemical reactions. Science 218, 747–754. www.jstor.org/stable/1689733.

Kumar, K.N., Ramesh, R., 2005. Synthesis, luminescent, redox and catalytic properties of Ru(II) carbonyl complexes containing 2N$_2$O donors. Polyhedron 24, 1885–1892. https://doi.org/10.1016/j.poly.2005.05.020.

Leyla, P., İlhami, G., Ahmet, C.G., Jacek, N., Alma, L., Shela, G., 2015. LC–MS/MS analysis, antioxidant and anticholinergic properties of galanga (Alpinia officinarum Hance) rhizomes. Ind. Crops Prod. 74, 712–721. https://doi.org/10.1016/j.indcrop.2015.05.034.

Li, B., Xu, Z., 1999. One-dimensional chain copper complexes [Cu(dien)(btrz)(ClO4)$_2$] and [Cu(en)$_2$(btrz)(ClO4)$_2$] based on the bridging ligand 1,2-bis(1,2,4-triazole-1-yl)ethane (btrz). Trans. Met. Chem. 24, 622–627. https://doi.org/10.1023/A:1006988716200.

Loncle, C., Brunel, J.M., Vidal, N., Dherbomez, M., Letourneux, Y., 2004. Synthesis and antifungal activity of cholesterol-hydrazone derivatives. Eur. J. Med. Chem. 39, 1067–1071. https://doi.org/10.1016/j.ejmech.2004.07.005.

Maravalli, P.B., Goudar, T.R., 1978. Substituted salen and baen tetradentate Schiff-base ligands. Synthesis, characterization, and electrochemistry of cobalt(III) complexes. Inorg. Chem. 17, 3389–3398. https://doi.org/10.1021/ic50190a018.

Majumder, A., Rosair, G.M., Mallick, A., Chattopadhyay, N., Mitra, S., 2006. Synthesis, structures and fluorescence of nickel, zinc and cadmium complexes with the N, N, O-tridentate Schiff base N-2-pyridylmethylidene-2-hydroxy-phenylamine. Polyhedron 25, 1753–1762. https://doi.org/10.1016/j.poly.2005.11.029.

Mehmet, S., Metin, C., Ismet, B., 2010. Synthesis, spectroscopic and biological studies on the new symmetric Schiff base derived from 2,6-diformyl-4-methylphenol with N-aminopyrimidine. J. Eur. Med. Chem. 45, 1935–1940. https://doi.org/10.1016/j.ejmech.2010.01.035.

Mishra, A.P., Mishra, R.K., Shrivastava, S.P., 2009. Structural and antimicrobial studies of coordination compounds of VO(II), Co(II), Ni(II) and Cu(II) with some Schiff bases involving 2-amino-4-chlorophenol. J. Serb. Chem. Soc. 74, 523–535. https://doi.org/10.2298/JSC0905523M.

Mohamed, G., El-Ghamrya, H.A., Shaimaa, K.F., Mohamed, A.M., 2018. Synthesis, spectroscopic, thermal and molecular modeling studies of Zn2+, Cd2+ and UO22+ complexes of Schiff bases containing triazole moiety.Antimicrobial, anticancer, antioxidant and DNA binding studies. Mater. Sci. Eng., C 83, 78–89. https://doi.org/10.1016/j.msec.2017.11.004.

Mohamed, H.H., Mohamed, A.S., Mohamed, E.G., Aljahdali, M., 2013. Synthesis and biological evaluation of some novel thiazole compounds as potential anti-inflammatory agents. Eur. J. Med. Chem. 65, 517–526. https://doi.org/10.1016/j.ejmech.2013.04.005.

Mohamed, G., Nadia, A., Hoda, E., Shaimaa, K.F., 2014. Synthesis, spectroscopic characterization, DNA interaction and biological activities of Mn(II), Co(II), Ni(II) and Cu(II) complexes with [(1H–1,2,4-triazole-3-ylimino)methyl]naphthalene-2-ol. J. Mol. Struct. 1076, 251–261. https://doi.org/10.1016/j.molstruc.2014.06.071.

Morsy, M.A., Tahani, I.K., Samar, A.A., 2011. Spectrochemical study and effect of high energatic gamma ray on copper (II) complexes. J. Solid State Sci. 13, 2080–2085. https://doi.org/10.1016/j.solidstatesciences.2011.07.015.

Najma, S., Asia, N., Bushra, K.B., Arayne, M.S., Mesaik, M.A., 2010. Synthesis, characterization, antibacterial, antifungal, and immunomodulating activities of gatifloxacin derivatives. Med. Chem. Res. 19, 1210–1221. https://doi.org/10.1007/s00044-009-9264-y.

Naidu, P.V.S., Kinthada, P.M.S., Murthy, Y.L.N., 2011. A novel method of synthesis of certain indole-3-aldehydes and their thiosemicarbazones as potential anticancer drugs. Int. J. Pharm. Biomed. Sci. 2, 92–98.

Nursen, S., Perihan, G., 2004. Some novel amino acid-schiff bases and their complexes synthesis, characterization, solid state conductivity behaviors and potentiometric studies. Z. Naturforsch. 59b, 692–698.

Nuraniye, E., Umit, M., Parham, T., Mehmet, A., Mehmet, T., İlhami, G., 2019. Screening the in vitro antioxidant, antimicrobial, anti-cholinesterase, antidiabetic activities of endemic Achillea cucullata (Asteraceae) ethanol extract. S. Afr. J. Bot. 120, 141–145. https://doi.org/10.1016/j.sajb.2018.04.001.

Rathinam, A., Sankaran, K.R., 2015. Design, synthesis, computational calculation and biological evaluation of some novel 2-thiazolyl hydrazones. Spectrochim. Acta A 135, 984–993. https://doi.org/10.1016/j.saa.2014.06.160.

Recio Despaigne, A.A., Parrilha, G.L., Izidoro, J.B., Da Costa, P.R., Dos Santos, R.G., Piro, O.E., Castellano, E.E., Rocha, W.R., Beraldo, H., 2012. 2-acetylpyridine- and 2-benzoylpyridine-derived hydrazones and their gallium(III) complexes are highly cytotoxic to glioma cells. Eur. J. Med. Chem. 50, 163–172. https://doi.org/10.1016/j.ejmech.2012.01.051.

Recio-Despaigne, A.A., Da Costa, F.B., Piro, O.E., Castellano, E.E., Louro, S.R.W., Beraldo, H., 2012. Complexation of 2-acetylpyridine- and 2-benzoylpyridine-derived hydrazones to copper(II) as an effective strategy for antimicrobial activity improvement. Polyhedron 38, 285–290. https://doi.org/10.1016/j.poly.2012.03.017.

Samar, A.A., 2017. Synthesis, characterization, and antitumor activity of new copper(I) and mercury(II) complexes. Russ. J. General Chem. 87, 1256–1263. https://doi.org/10.1134/S1070363217060214.

Samar, A.A., Hanaa, A.E., 2019. Effect of gamma irradiation on Spectral, XRD, SEM, DNA binding, molecular modling and antibacterial property of some (Z)-N-(furan-2-yl)methylene)-2-(phenylamino)acetohydrazide metal(II) complexes. J. Mol. Stru. 1185, 323. https://doi.org/10.1016/j.molstruc.2019.02.069.

Saeed, A., Najma, S., Urooj, H., Mesaik, M., 2009. Synthesis, characterization, antibacterial and anti-Inflammatory activities of enoxacin metal complexes. Bioinorg. Chem. Appl. 2009, 1–6. https://doi.org/10.1155/2009/914105.

Savini, L., Chiasserini, L., Travagli, V., Pellerano, C., Novellino, E., Cosentino, S., Pisano, M.B., 2004. New alpha-(N)-heterocyclichydrazones: evaluation of anticancer, anti-HIV and antimicrobial activity. Eur. J. Med. Chem. 39, 113–122. https://doi.org/10.1016/j.ejmech.2003.09.012.

Seda, S., Baybars, K., Fatma, K., Sevgi, H.B., 2009. Theoretical and spectroscopic studies of 5-fluoro-isatin-3-(N-benzylthiosemicarbazone) and its zinc(II) complex. J. Mol. Struct. 917, 63–70. https://doi.org/10.1016/j.molstruc.2008.06.033.

Shankarwar, S.G., Nagolkar, B.B., Shelke, V.A., Chondhekar, T.K., 2015. Synthesis, spectral, thermal and antimicrobial studies of transition metal complexes of 14-membered tetraaza[N_4] macrocyclic ligand. Spectrochim. Acta A 145, 188–193. https://doi.org/10.1016/j.saa.2015.02.006.

Sherif, E.M., Ahmed, A.H., 2010. Synthesizing new hydrazone derivatives and studying their effects on the inhibition of copper corrosion in sodium chloride solution. Synth. React. Inorg. Met.-Org. Nano-Metal Chem. 40, 365–372. https://doi.org/10.1080/15533174.2010.492546.

Sun, L., McMahon, G., 2000. Inhibition of tumor angiogenesis by synthetic receptor tyrosine kinase inhibitors. Drug Discov. Today 5, 344–353. https://doi.org/10.1016/S1359-6446(00)01534-8.

Shah, R., 2016. Ligational, potentiometric and floatation studies on Cu(II) complexes of hydrazones derived from p and o-vanillin condensed with diketo hydrazide. J. Mol. Liq. 220, 939–953. https://doi.org/10.1016/j.molliq.2016.04.047.

Turuvekere, K.C., Kikkeri, N.M., Doddahosuru, M.G., Harmesh, C.T., 2016. Inhibition activity of new thiazole hydrazones towards mild steel corrosion in acid media by thermodynamic, electrochemical and quantum chemical methods. Taiwan Inst. Chem. Eng. 67, 521–531. http://dx.doi.org/10.1016%2Fj.jtice.2016.08.013.

Tweedy, B.G., 1964. Plant extracts with metal ions as potential antimicrobial agents. Phytopathology 55, 910–914.

Vinodkumar, C.R., Nair, M.K., Radhakrishnan, P.K., 2000. Thermal studies on lanthanide nitrate complexes of 4-n-(2'-furfurylidene) aminoantipyrine. J. Therm. Anal. Cal. 61, 143–149. https://doi.org/10.1023/A:1010120909987.

Wikler, M.A., Cockerill, F.R., Bush, K., Dudley, M.N., Eliopoulos, G.M., Hardy, D.J., Hecht, D.W., Ferraro, M.J., Swenson, J.M., Hindler, J.F., Patel, J.B., Powell, M., Turnidge, J.D., Weinstein, M.P., Zimmer, B.L., 2009. Pennsylvania 29 (2), 1087-.

Xavier1, D.A., Srividhya, N., 2014. Synthesis and study of schiff base ligands. J. Appl. Chem. 7, 6–15. http://www.iosrjournals.org.

Yin, H.D., Chen, S.W., 2006. Synthesis and characterization of di- and tri-organotin(IV) complexes with Schiff base ligand pyruvic acid 3-hydroxy-2-naphthoyl hydrazone. Inorg. Chim. Acta 359, 3330–3338. https://doi.org/10.1016/j.ica.2006.03.024.

Yusuff, K.M., Sreekala, R., 1990. Thermal and spectral studies of 1-benzyl-2- phenylbenzimidazole complexes of cobalt(II). Thermochim. Acta 159, 357–368. https://doi.org/10.1016/0040-6031(90)80121-E.

Yousef, T.A., Abu El-Reash, G.M., Al-Jahdali, M., El-Bastawesy, R., Rakhawy, El-, 2013. Structural and biological evaluation of some metal complexes of vanillin-4N-(2-pyridyl) thiosemicarbazone. J. Mol. Struct. 1053, 15–21. https://doi.org/10.1016/j.molstruc.2013.08.034.

Yousef, T.A., Abu El-Reash, G.M., El-Bastawesy, R., El-Rakhawy, 2014. Structural, spectral, thermal and biological studies on (E)-2-(1-(4-hydroxyphenyl)ethylidene)-N-(pyridin-2-yl)hydrazinecarbothioamide and its metal complexes. Spectrochim. Acta A Mol. Biomol. Spectrosc. 133, 568–578. https://doi.org/10.1016/j.saa.2014.05.041.

Yousef, T., Rakha, T., El Ayaan, U., Abu El Reash, G., 2012. Synthesis, spectroscopic characterization and thermal behavior of metal complexes formed with (Z)-2-oxo-2-(2-(2-oxoindolin-3-ylidene)hydrazinyl)-N-phenylacetamide (H_2OI). J. Mol. Struct. 1007, 146–157. https://doi.org/10.1016/j.molstruc.2011.10.036.

Yousef, T., El-Reash, G.A., Attia, M., El-Tabai, M., 2015. Comparative ligational, optical band gap and biological studies on Cr(III) and Fe(III) complexes of hydrazones derived from 2-hydrazinyl-2-oxo-N-phenylacetamide with both vanillin and O-vanillin. Chem. Phys. Lett. 636, 180–192. https://doi.org/10.1016/j.cplett.2015.07.001.